ECMWF System 4 forecasts for Malaria in Malawi

This analysis employs the European Centre for Medium Range Weather Forecasting (ECMWF) System 4 hindcast ensemble of 15 members starting on the 1st of every month for the years 1981-2010, and run for 7 months. The system consists of an initial ocean analysis to estimate the initial state of the ocean and a global coupled ocean-atmosphere general circulation model to calculate the evolution of the ocean and atmosphere. Daily temperature and precipitation from the System 4 ensemble are then used to drive the Liverpool Malaria Model (LMM), with a one-year spin up period driven by ERA-Interim climatological values for Africa. The output is compared to various sets of gridded climatological products:

- Temperature observations from the Climate Research Unit (CRUT3.1, Mitchell and Jones, 2005) covering the period 1950-2009.
- Mixed satellite and rain gauges observations from the Global Precipitation Climatology Project (GPCP) dataset (Huffman et al, 2001). Monthly values are available for rainfall between 1979 and 2010, however daily values required to drive LMM were only available between 1997 and 2008.
- Mixed satellite and rain gauges observations from the NASA Goddard Space Flight Center Tropical Rainfall Measuring Mission (TRMM) dataset (Huffman et al, 2001) for 1998-2010.
- Temperature and rainfall products based on NCEP-NCAR (1948-2010, Kalnay et al, 1996) and ERA Interim for (ERAI, 1979-2011, Uppala et al, 2008) reanalyses (blend of climate model outputs and various sources of observations using complex assimilation methods).

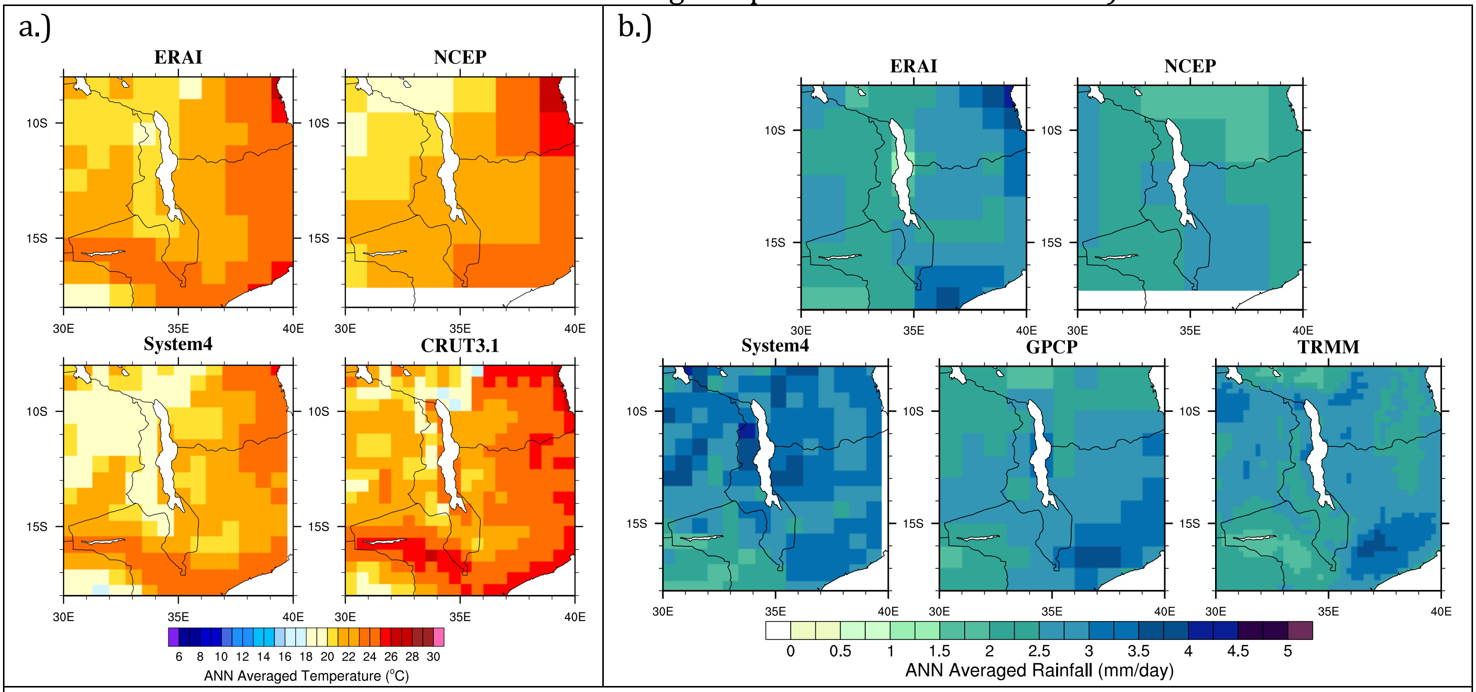

Figure 1: Annual average a.) temperature and b.) precipitation for Malawi. System 4 forecasts take the fourth month forecasted from each start date (see table 1 for explanation).

The annual averages for System 4 (forecast month 4, see table 1 for explanation) compare reasonably well with the climatological values, with cooler temperatures in the northwest and warmer temperatures in the south and east (compare NCEP and System 4 in Fig.1a) but a few degrees cooler overall compared to the observations (CRUTS). Annual averaged rainfall is elevated near the Mozambique Channel in all datasets and the System 4 forecast (Fig.1b). However, System 4 appears to be particularly wet in the annual average over much of northern Malawi compared to the hybrid satellite/model climatologies of GPCP and TRMM and the climatological reanalyses ERAI and NCEP.

The seasonal cycles of temperature and precipitation (Fig.2, averaged exclusively over Malawi) show a distinct pattern of cool temperatures and low rainfall in the middle of the year in JJA and vice versa, with peak temperatures occurring in SON, just before the peak rainfall season occurring in DJF. Elevated rainfall is consistently suggested by System 4 forecasts (see Fig.1b), although with longer forecast lead times, the deviation from the data products, which tend to agree fairly well, is reduced.

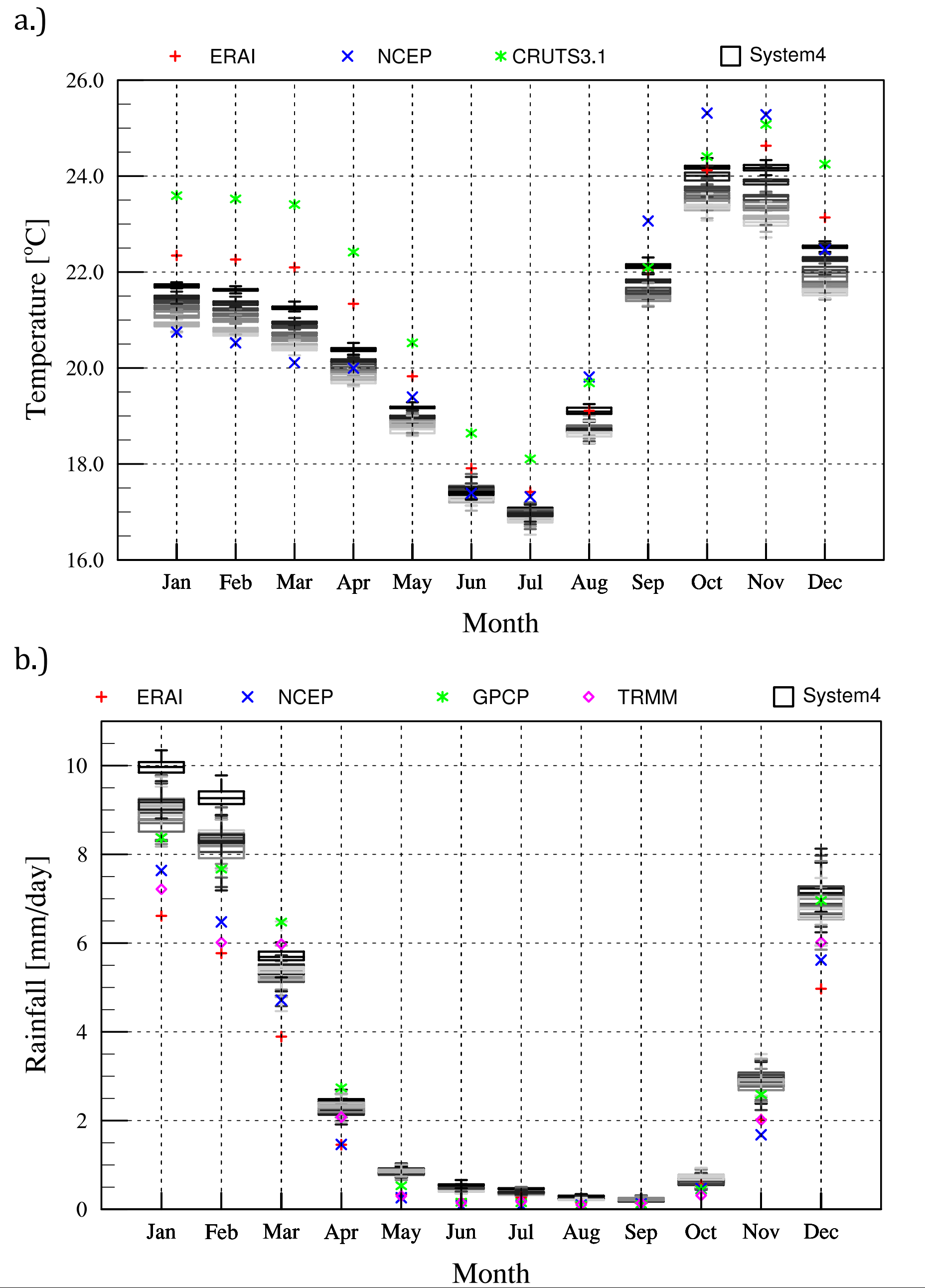

Figure 2: Seasonal cycle of (a.) temperature and (b.) precipitation in Malawi, masked using the Database of Global Administrative Areas (GADMv2.1). System 4 forecasts are shown as box and whisker plots for forecast months 1 to 7 (black – light grey) for the lower tercile, mean and upper tercile values.

There is relatively small spread in System 4 forecast distances of 1 to 7 months from the start date (see Table 1).

Table 1: Illustration of the System 4 seasonal forecast scheme. Each System 4 forecast is seven months long, with a start date in each month of the year. The “Forecast month” is the distance in time from the in initial conditions with 1 being the first month of the forecast (same month as the start date) and 7 being the final month of the forecast. To build a timeseries, we chose the value for “Forecast month” and extract that month’s data from each start date. For example, for Forecast month = 1, we take Jan from the first start date in 1981, Feb from the second start date in 1981, etc. For Forecast month = 7, we take Jul from the first start date in 1981, Aug from the second start date in 1981, etc. When Forecast month > 1, the timeseries extends into 2011 since the last start date (12) in 2010 gives Dec when Forecast month=1, Jan when Forecast month=2 to Jun when Forecast month=7.

Forecast month	1981												…	2010			2011					
1	J	F	M	A	M	J	J	A	S	O	N	D	…	J	…	D						
2		F	M	A	M	J	J	A	S	O	N	D	…	J	…	D	J					
…	…	…	…	…	…	…	…	…	…	…	…	…	…	…	…	…	…	…	…	…	…	…
6						J	J	A	S	O	N	D	…	J	…	D	J	F	M	A	M	
7							J	A	S	O	N	D	…	J	…	D	D	F	M	A	M	J

Average DJF distributions of temperature and rainfall (Fig.3) again compare well with the other datasets, although the System 4 forecast is considerably wetter in Malawi (Fig.2b) and eastern Zambia, although TRMM does also indicate elevated rainfall in this region.

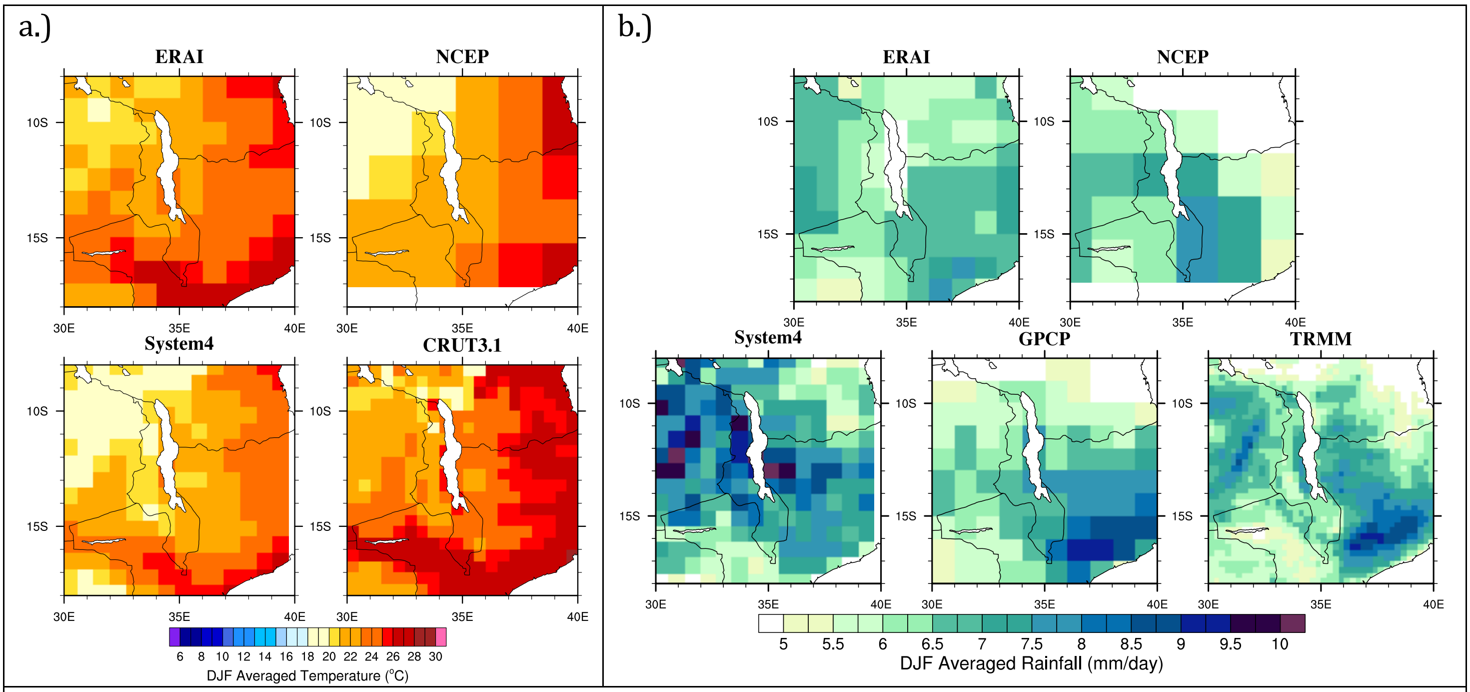

Figure 3: DJF average a.) temperature and b.) precipitation for Malawi. System 4 forecasts use a four-month lead time using February start dates for an DJF target.

The seasonal cycle of malaria in Malawi, simulated by the Liverpool Malaria Model (LMM) forced by climatological data (Fig.4), shows a pronounced increase in malaria incidence between February and March, with fairly consistent levels in MAM and a gradual decline between June and August. System 4 forecasts only a short distance from initialisation tend to start with high incidence, in agreement with ERAI, GPCP and TRMM climatologies, and then decline towards the NCEP climatology, which is consistently low compared to the other sources of data.

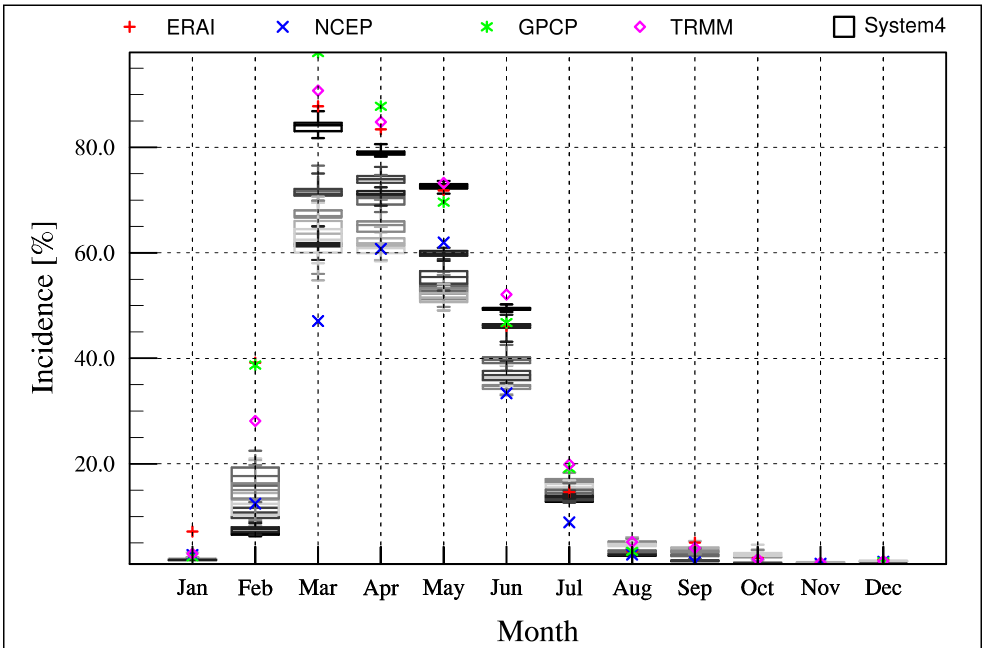

Figure 4: Seasonal cycle of malaria incidence in Malawi, masked using the Database of Global Administrative Areas (GADMv2.0). System 4 forecasts are shown as box and whisker plots for forecast months 1 to 7 (black – light grey) for the lower tercile, mean and upper tercile values.

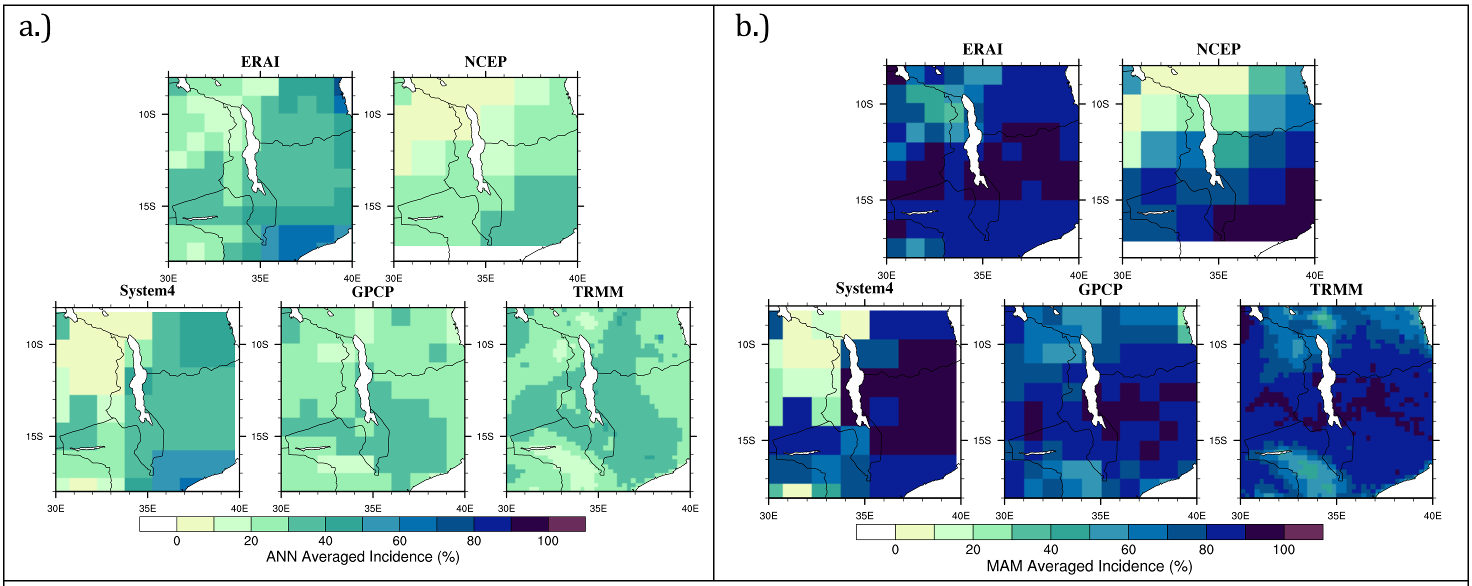

Figure 5: Malaria Incidence a.) annually averaged and b.) averaged over the peak malaria season MAM. System 4 forecasts use a four-month lead time using May start dates for an MAM target.

The distribution of malaria incidence is comparable across the range of temperature and rainfall products used to drive the model in the annual average (Fig.5a), with low incidence to the west of Lake Malawi and higher incidence to the west. For the MAM peak incidence season (Fig.5b), malaria occurrence shows a peak band stretching across the centre of the region at roughly 13°S in ERAI, GPCP and TRMM, except for the NCEP reanalysis, which actually suggests lower incidence in this location. System 4 only partially captures this feature, largely in the neighbouring Mozambique.

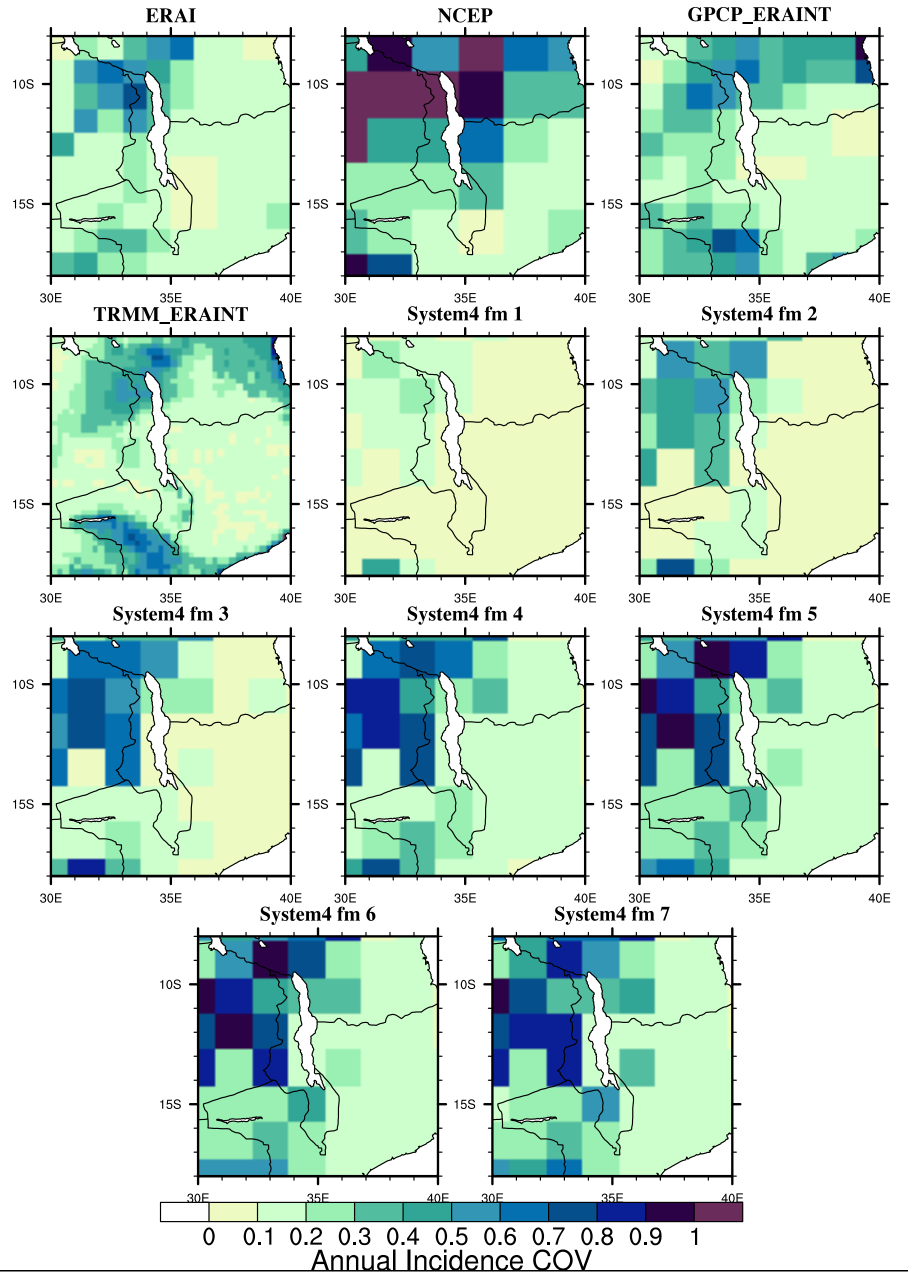

Figure 6: Malaria incidence coefficient of variation (COV) which is the standard deviation divided by the annual mean for the datasets driving LMM. System 4 values are shown for each month of the forecast.

The epidemic fringe (Fig.6), the region of highest Interannual variability in malaria incidence lies across the northern part of Malawi and off to the southwest in Mozanbique in ERAI, NCEP, GPCP and TRMM. System 4 values suggest that most forecast lead times, except for the first capture the high interannual variability of malaria incidence in the northwest of the region.

The same diagnostic, repeated for only the peak malaria season (MAM) with a four month System 4 forecast lead time produces a similar result with the epidemic fringe in the north of Malawi highlighted in all datasets, as well as high variability in the south of Malawi in GPCP, TRMM and System 4 (Fig.7).

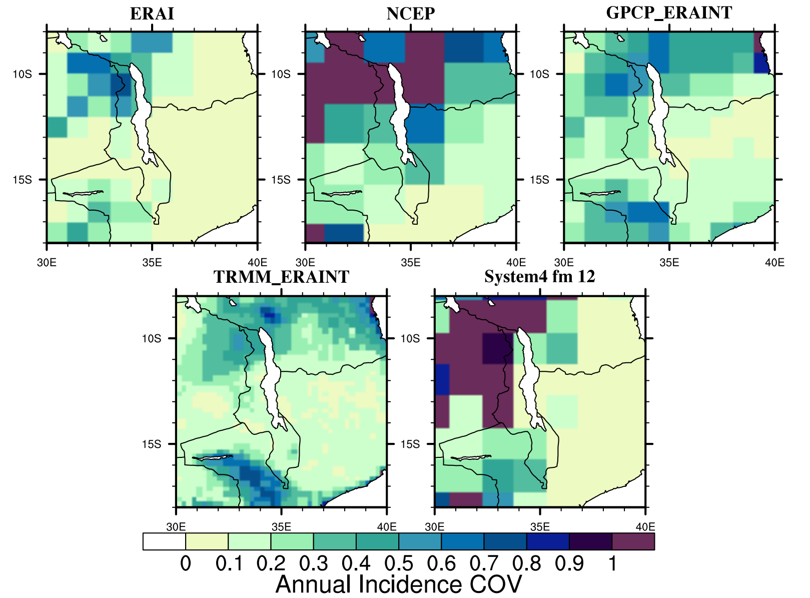

Figure 7: Malaria incidence coefficient of variation (COV) which is the standard deviation divided by the MAM mean for the datasets driving LMM. System 4 values use a four-month lead-time using December (fm 12) start dates for an MAM target.

Interannual variability of temperature, precipitation and malaria incidence averaged over Malawi for the peak malaria season (MAM) are shown in Fig.8, with the System 4 forecasts taken with increasing lead times from the target season, allowing five realisations (see table 2 for explanation).

Table 2: Illustration of the different System 4 forecast start dates used for the two target seasons to calculate interannual variability and Relative Operating Characteristics (ROC) curve areas at several forecast lead times. Three month seasonal averages could not be computed for lead times of 6 and 7 months.

Forecast Month (fm)	1	2	3	4	5	6	7
DJF Target Start Date	5 (May)	4 (Apr)	3 (Mar)	2 (Feb)	1 (Jan)	12 (Dec)	11 (Nov)
MAM Target Start Date	8 (Aug)	7 (Jul)	6 (Jun)	5 (May)	4 (Apr)	3 (Mar)	2 (Feb)
Target Months	1-3	2-4	3-5	4-6	5-7	N/A	N/A

Interannual variability (Fig.8) for temperature is reasonably well captured by System 4 forecasts, even at short forecast lead times, with particularly good correspondence with the CRUTS observational data. However, for long range forecasts of 5 months Sysem 4 appears to perform poorly, especially in the MAM season. The variability within the ERAI dataset is sometimes missed by the System 4 forecasts, while the NCEP climatology often lies outside the forecast ensemble tercile range in DJF but seems to perform consistently better in MAM. System 4 forecasts also do not perform particularly well in Interannual variability for precipitation against the other datasets, particularly in DJF, although there is considerable scatter between climatologies. Despite this, the interannual variability in malaria incidence in MAM appears to agree between System 4 forecasts, ERAI, GPCP and TRMM datasets, whilst the variability produced by the NCEP climatology is to high.

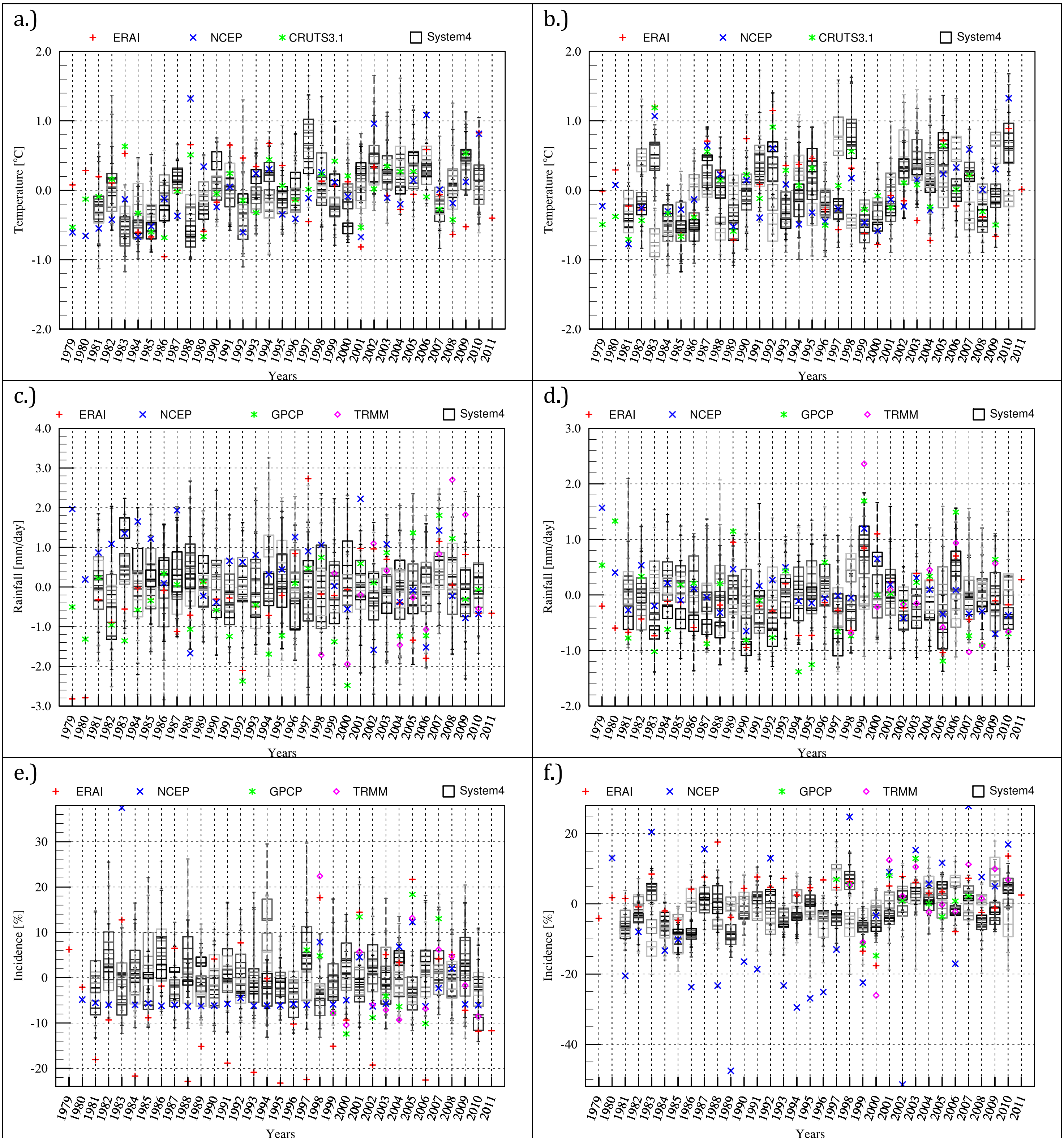

Figure 8: Interannual variability of (a,b) temperature, (c,d) precipitation and (e,f) malaria incidence for the peak rainfall season (DJF, left column) and the peak malaria season (MAM, right colomn). The values are anomalies with a mean value subtracted that is calculated as the multi-year mean of each data product over their common, overlapping window of data availability. System 4 forecasts are plotted with increasing forecast start date lead times from 1 (black) to 5 (light grey) – see table 2 for details.

Skill in the System4 forecasts is determined by computing the geometrical area under the Relative Operating Characteristics (ROC) curve at each grid point for below lower tercile events, above median events and above upper tercile (extreme) events compared to the other climatologies. For perfect forecasts, all ensemble members will correctly predict an event (or non-event) in all years with a ROC area under the curve of 1.0, the maximum possible value. Forecasts with little or no skill that perform no better than climatology return ROC areas of less than 0.5. ROC areas were calculated for targets of the three-month peak rainfall season (DJF) and the peak malaria season (MAM), with 5 increasing forecast lead times (see table 2).

The significance of these values can be determined by performing a two-tailed Mann-Whitney U-statistic test, using a look-up table referencing the number of events and non-events, and calculating a critical ROC area value that must be exceeded. For example, upper tercile events, with a probability of 33%, in a 30-year timeseries, should produce 10 events (N_e) and 20 non-events (N_n). At the 95% confidence level, the critical U value from a reference table is 55, giving a ROC area of $0.5+U/(N_eN_n) = 0.775$. Calculated ROC scores comparing upper tercile events in 30 years of data that exceed 0.775 are therefore significant where $p<0.05$.

There is a significant skill in forecasting MAM temperatures in Malawi compared to the three climatological datasets (Fig.9) in the first three forecast lead times after which forecast skill is no better than climatology. The System 4 forecasts are noticeably less skillful compared to the NCEP climatology.

Contrary to this, there appears to be little skill in the System 4 forecasts of DJF rainfall (Fig.10) compared to climatology. Nevertheless, some parts of forecasts compared to TRMM are significantly skillful across parts of Tanzania. The situation is similar for forecasts of MAM rainfall (Fig.11), where the forecasts show some skill in northern Mozambique and southern Tanzania.

ROC skill for malaria incidence in MAM (Fig.12) should be interpreted in conjunction with geographical incidence variability (Fig.6 and 7) since the useful skill occurs in regions of high interannual variability where epidemics are possible. With this in mind, the System 4 forecasts do actually appear to be skillful in north Malawi compared to ERAI, NCEP and TRMM, for the first three seasonal realization, although there might be moderate skill in when compared to GPCP although this is fairly patchy and only significant in isolated regions.

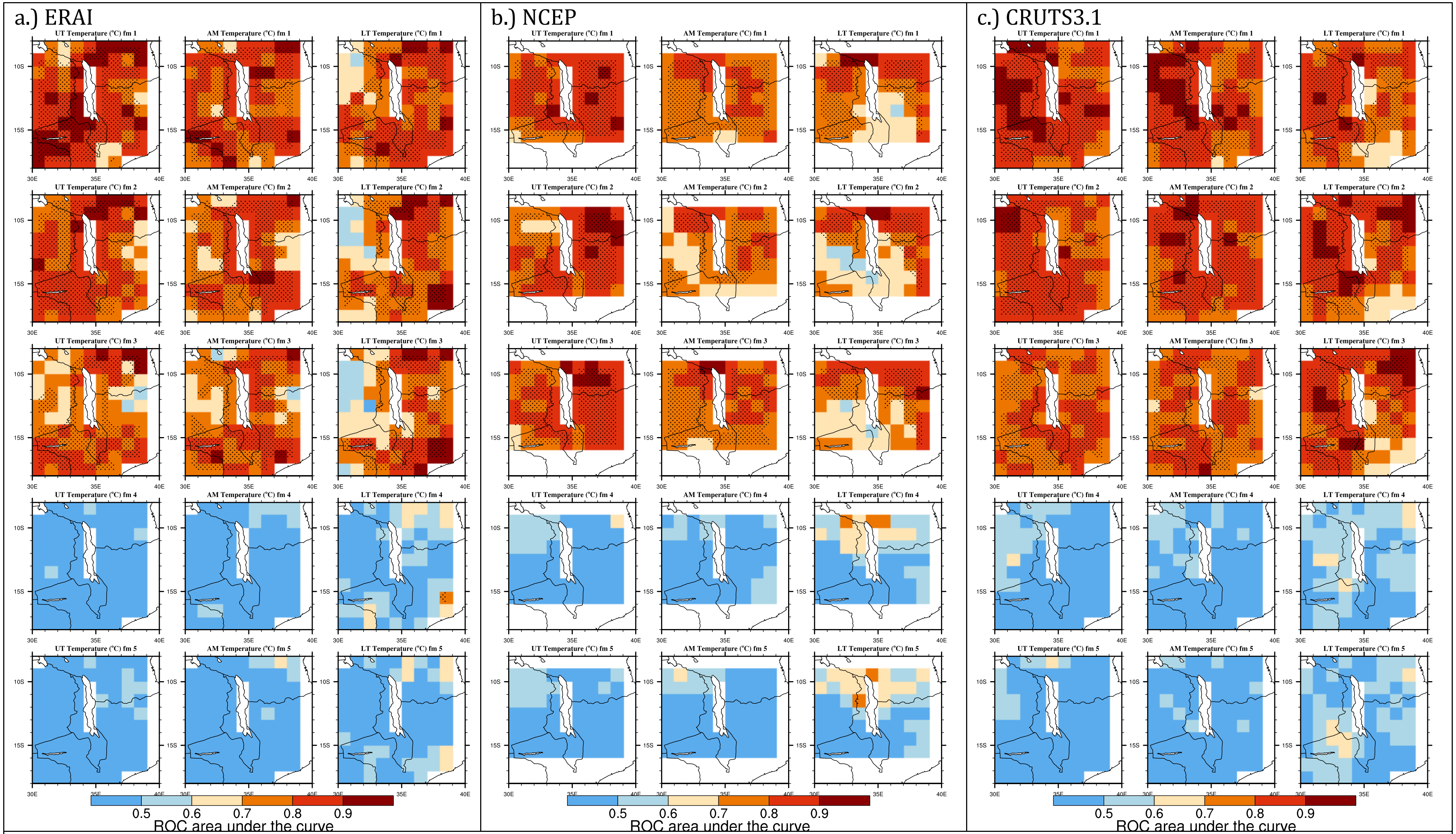

Figure 9: Relative Operating Characteristics (ROC) areas under the curve for MAM season temperature forecast skill for above upper tercile (extreme) events (UT, left column), above median events (AM, central column) and below lower tercile events (LT, right column) compared to a.) ERAI, b.) NCEP and c.) CRUTS3.1 climatological data. The five different rows represent increasing forecast lead times from 1 month (top row) to 5 months (bottom row) of the target season (see table 2). Stippling indicates significance at the 95% confidence interval, calculated by performing a two-tailed Mann-Whitney U-statistic test.

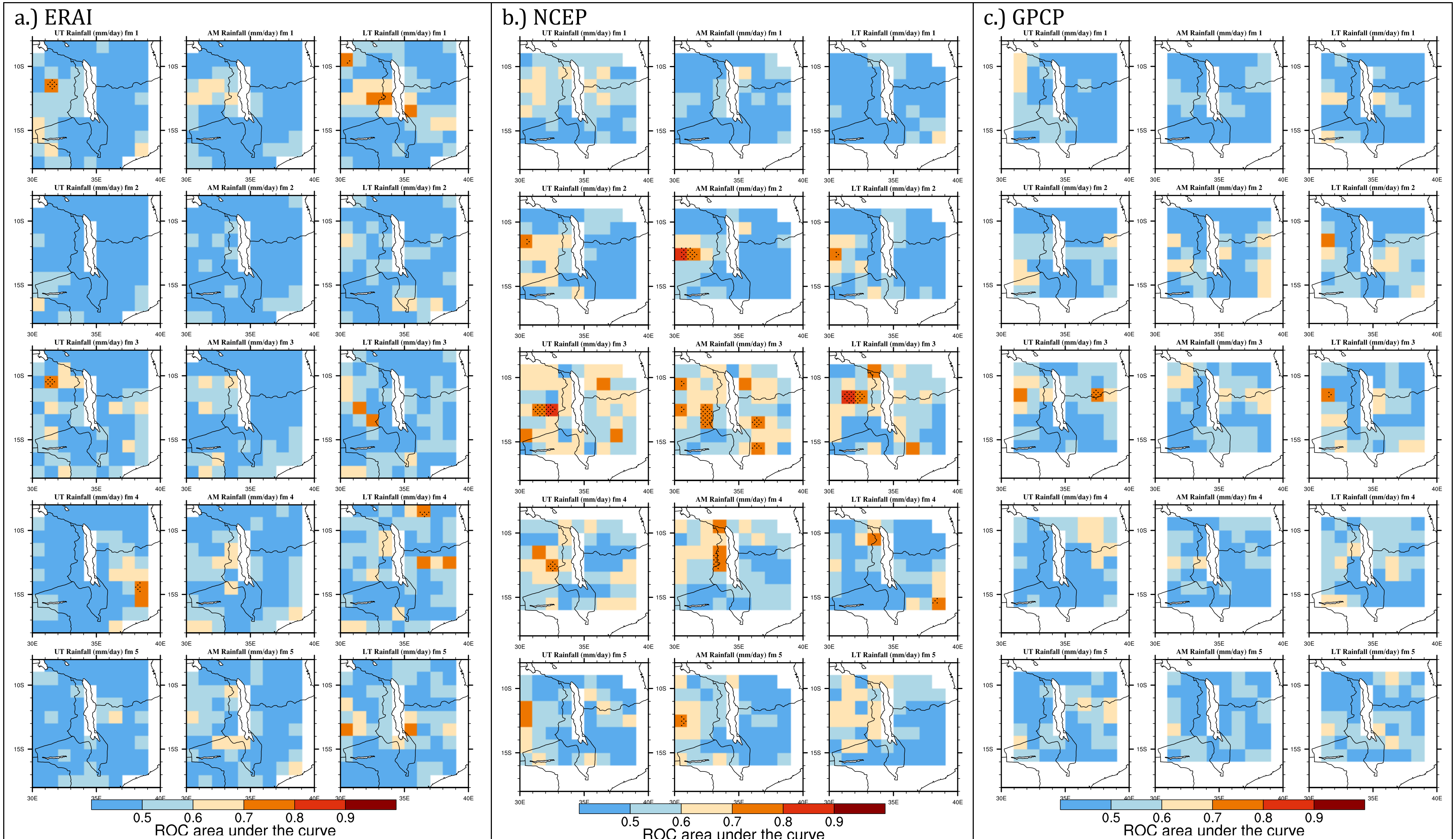

Figure 10: Relative Operating Characteristics (ROC) areas under the curve for DJF season rainfall forecast skill for above upper tercile (extreme) events (UT, left column), above median events (AM, central column) and below lower tercile events (LT, right column) compared to a.) ERAI, b.) NCEP, c.) GPCP and d.) TRMM climatological data. Data were masked by very low perecipitation (<1mm/day). The five different rows represent increasing forecast lead times from 1 month (top row) to 5 months (bottom row) of the target season (see table 2). Stippling indicates significance at the 95% confidence interval, calculated by performing a two-tailed Mann-Whitney U-statistic test.

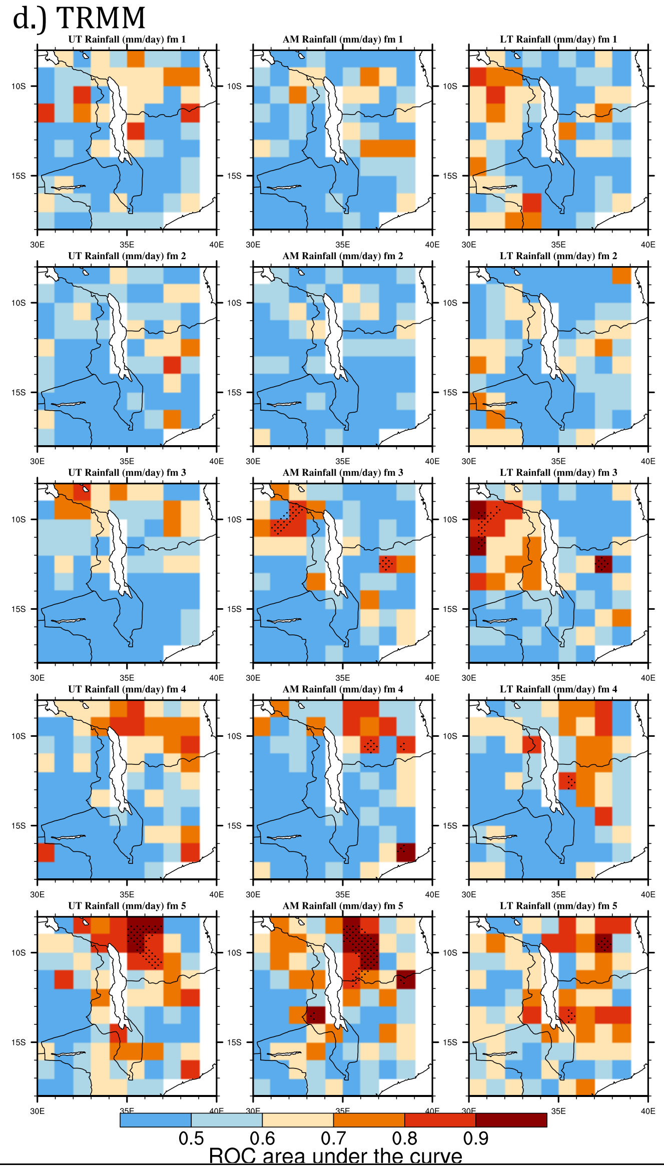

Figure 10, continued

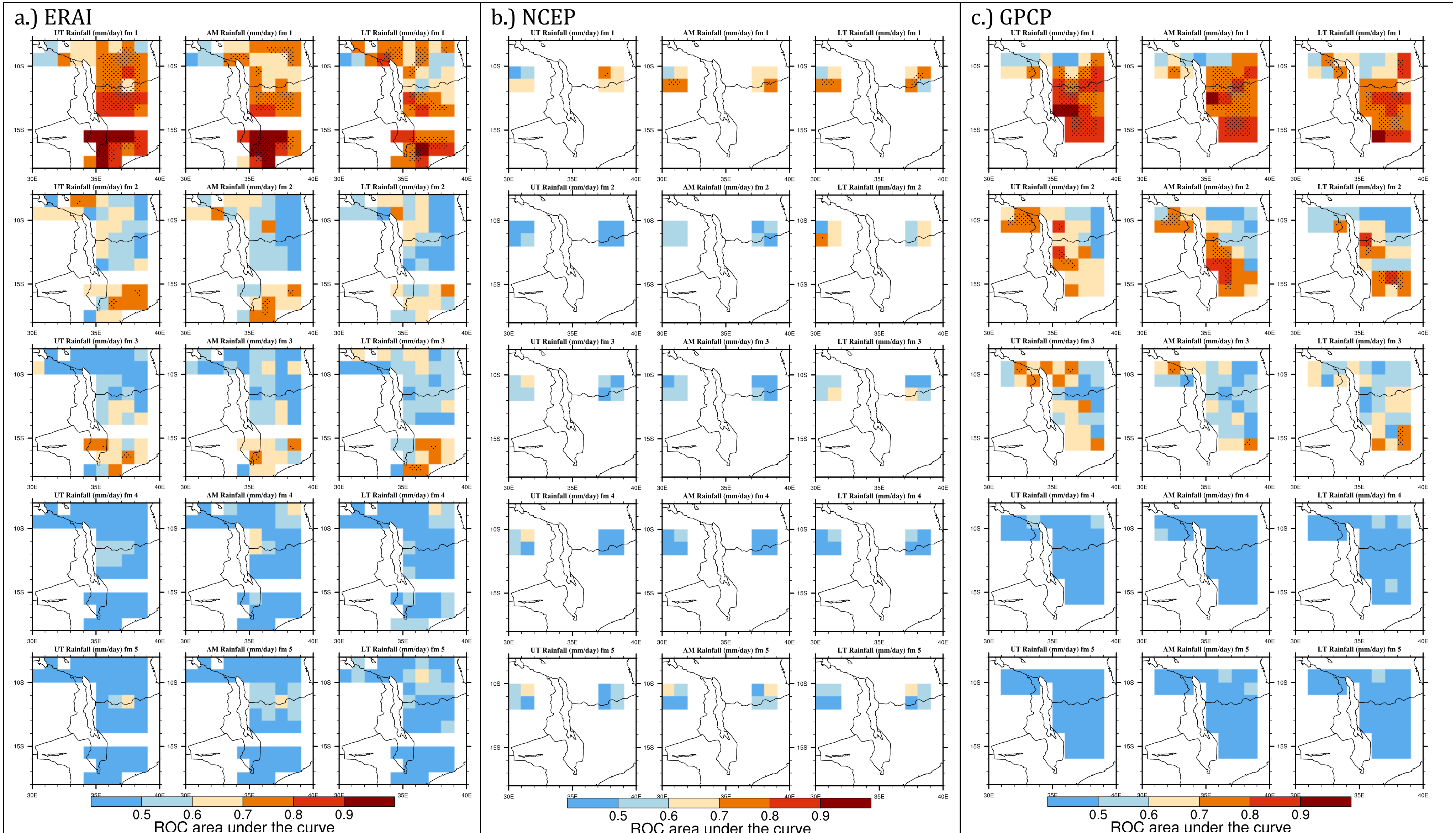

Figure 11: Relative Operating Characteristics (ROC) areas under the curve for MAM season rainfall forecast skill for above upper tercile (extreme) events (UT, left column), above median events (AM, central column) and below lower tercile events (LT, right column) compared to a.) ERAI, b.) NCEP, c.) GPCP and d.) TRMM climatological data. Data were masked by very low perecipitation (<1mm/day). The five different rows represent increasing forecast lead times from 1 month (top row) to 5 months (bottom row) of the target season (see table 2). Stippling indicates significance at the 95% confidence interval, calculated by performing a two-tailed Mann-Whitney U-statistic test.

d.) TRMM

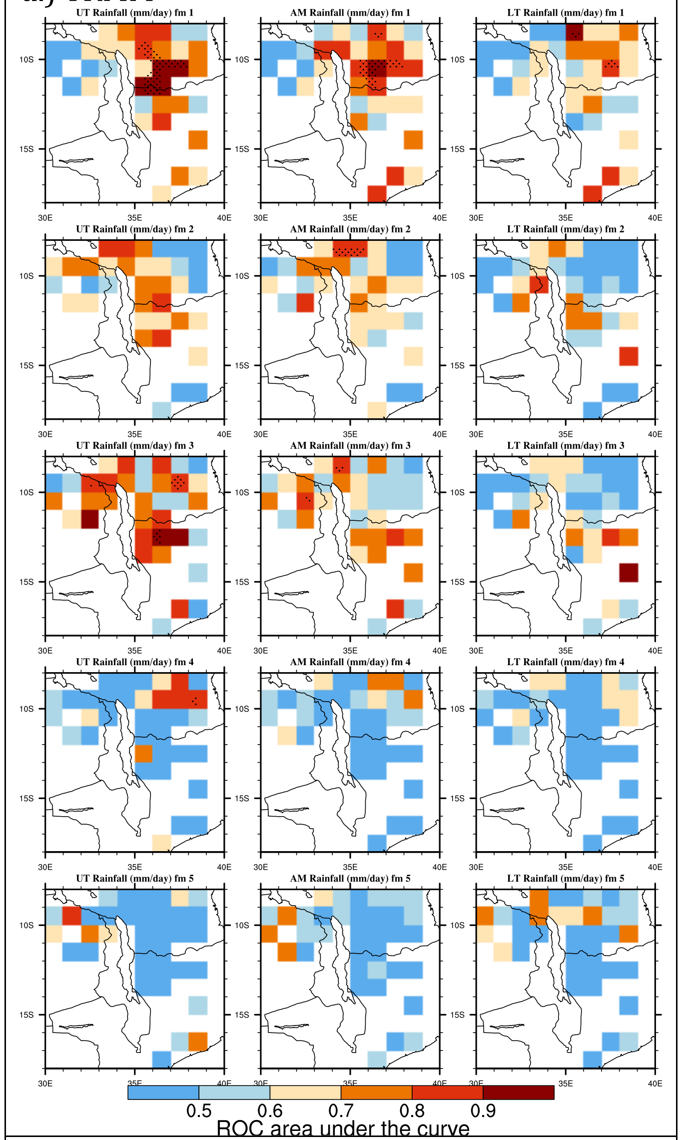

Figure 11, continued

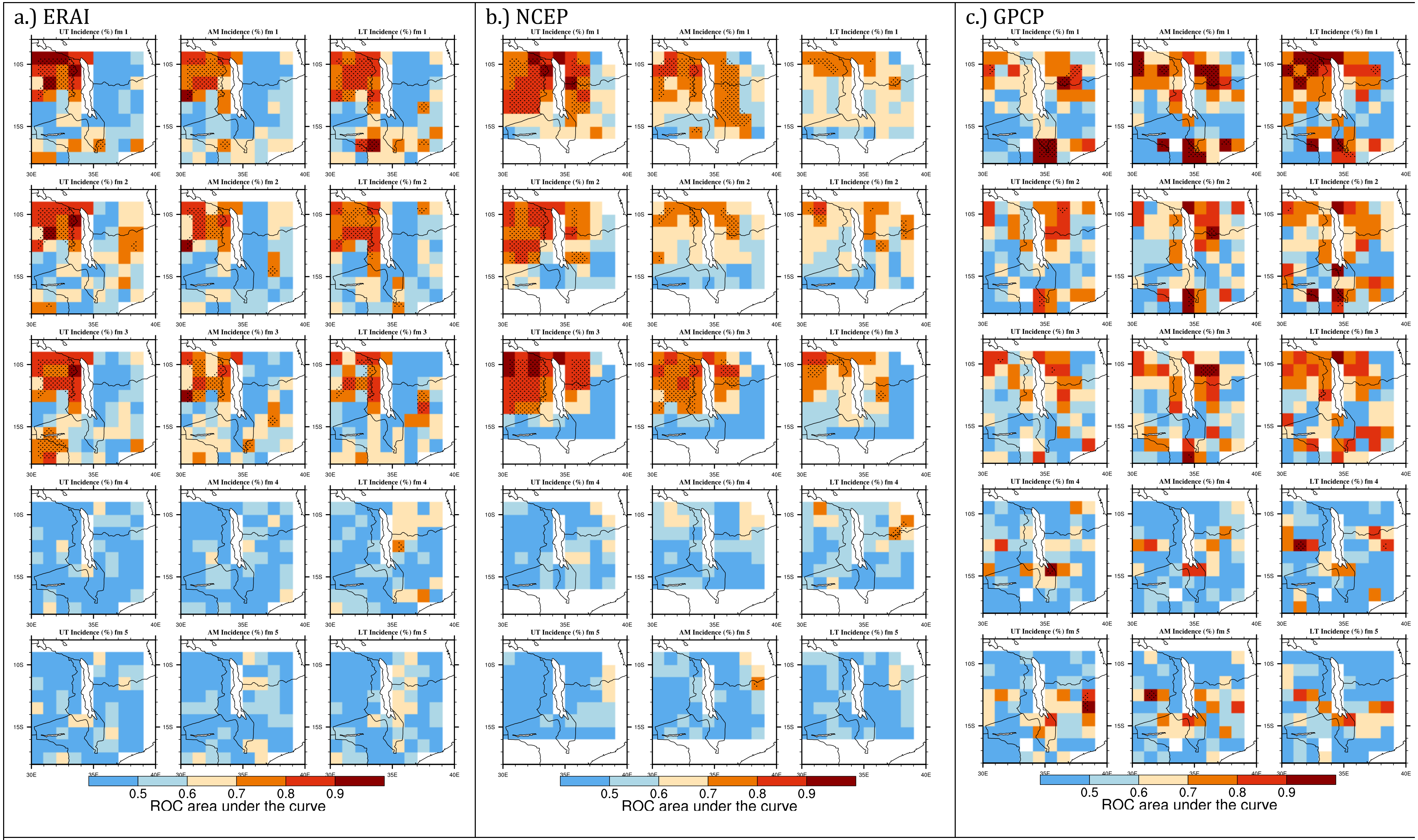

Figure 12: Relative Operating Characteristics (ROC) areas under the curve for MAM season malaria incidence forecast skill for above upper tercile (extreme) events (UT, left column), above median events (AM, central column) and below lower tercile events (LT, right column) compared to a.) ERAI, b.) NCEP, c.) GPCP and d.) TRMM climatological data. Data were masked by very low percipitation (<1%). The five different rows represent increasing forecast lead times from 1 month (top row) to 5 months (bottom row) of the target season (see table 2). Stippling indicates significance at the 95% confidence interval, calculated by performing a two-tailed Mann-Whitney U-statistic test.

d.) TRMM

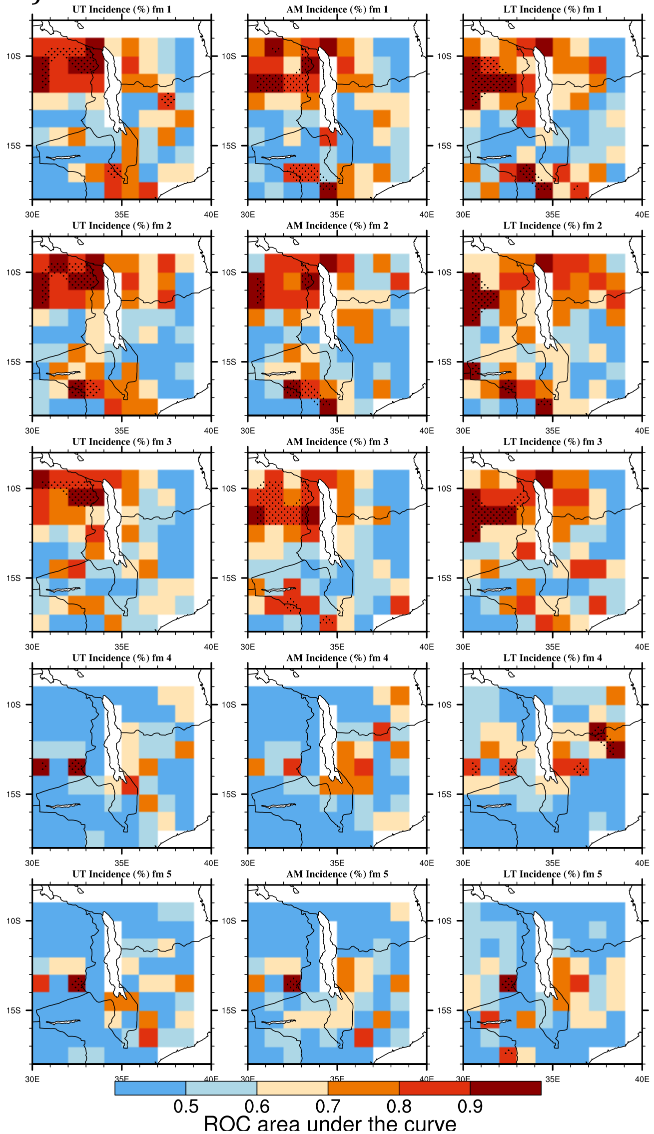

Figure 12, continued